Anion-Specific Partitioning in Two-Phase Finite Volume Systems: Possible Implications for Mechanisms of Ion Pumps

M. Boström,[†,‡,§] E. R. A. Lima,[⊥,#] E. C. Biscaia, Jr.,[⊥] F. W. Tavares,[*,#] P. Lo Nostro,[¶] D. F. Parsons,[▽] V. Deniz,[▽] and B. W. Ninham[▽]

Department of Physics, Chemistry and Biology, Linköping University, SE-581 83 Linköping, Sweden, Institute of Physical and Theoretical Chemistry, University of Regensburg, D-93040 Regensburg, Germany, Dipartimento di Scienze Chimiche, Universita di Cagliari-CSGI Cittadella Monserrato, S.S. 554 Bivio Sestu, 09042 Monserrato, Italy, Programa de Engenharia Química, COPPE, Universidade Federal do Rio de Janeiro, 21945-970, Rio de Janeiro, RJ, Brazil, Escola de Química, Universidade Federal do Rio de Janeiro, Cidade Universitária, CEP 21949-900, Rio de Janeiro, RJ, Brazil, Department of Chemistry and C.S.G.I., University of Florence, Via della Lastruccia 3, I-50019 Sesto Fiorentino (Firenze), Italy, and Research School of Physical Sciences and Engineering, Australian National University, Canberra, Australia 0200

Received: October 13, 2008; Revised Manuscript Received: March 17, 2009

In two-phase finite volume systems of electroneutral phospholipids, the electrolyte concentration is different in the two phases. The partitioning is highly anion-specific, a phenomenon not accounted for by classical electrolyte theories. It is explained if ionic dispersion forces that lead to specific ion binding are taken into account. The mechanism provides a contribution to active ion pumps not previously considered.

1. Introduction

Specific ion effects occur almost everywhere in biological and colloidal systems.[1] A classical example is the highly ion-specific Donnan equilibria of red blood cells.[2] Much higher concentrations of potassium ions occur inside of a red cell than outside and vice versa for sodium ions. A central issue in molecular biology is that this circumstance is due to active ion pumps. Theories of physical chemistry could not account for such phenomena; therefore, the need for some active biochemical transport mechanism seemed evident. The attribution of such ion specificity to active ion pumps is a central tenet of biology and hardly questioned.[3] A few[4] have maintained that the physical and biochemical evidence for pumps is slight. However, such opposition has not been taken seriously.

Our aim here is not to question the existence of ion pumps. However, we do wish to point out that the classical theories of physical chemistry of electrolytes, which lead logically to the inevitability of active ion pumps, are incomplete.[5] These theories attribute ionic interactions to electrostatic forces alone, be they between ions or of ions with membranes. The variously termed dispersion or Lifshitz forces include many-body quantum mechanical forces, dipole−dipole, dipole−induced dipole, and induced dipole−induced dipole interactions, neglected in standard theories of physical chemistry. Their proper inclusion in classical theory accounts for at least a large part of a host of Hofmeister or specific ion effects in chemistry. Classical theories ignore, or treat inadequately, forces of electrodynamic origin.[5−8] We have discussed in previous papers that Hofmeister effects, that is, bulk or interfacial phenomena where the strong specificity of a single electrolyte (and therefore that of a cation−anion pair) emerges, cannot be explained in terms of electrostatic (nonspecific) forces. Instead, dispersion (specific) forces must be taken into account.

In fact, while electrostatic Coulomb interactions depend on the charge and distance of the involved species only, dispersion forces are related to parameters such as polarizabilities and ionization potentials that derive from the electronic configuration of the ions and therefore express specificity.

Electrostatic theories, such as the Debye−Hückel theory, work quite well as limiting cases, that is, when the concentration of the ions is small (typically below, say, 1−10 mM). However, when the ionic strength rises close to classical physiological values (about 100 mM), then specificity emerges, and pure electrostatic models do not explain the experimental results. Hence, at very low concentration, electrostatic interactions prevail, and no sign of ion specificity can be traced. At higher concentrations, dispersion forces become dominant while electrostatic interactions are screened. This emerges clearly in the activity coefficients of aqueous salt solutions that reflect the ion−ion and ion−solvent interactions. As a matter of fact, the extended form of the Debye−Hückel equation includes a term (bI) that accounts for specific interactions between the ions and the solvent, $\log \gamma_{\pm} = [-(A|z_+z_-|(I)^{1/2})/(1 + Ba(I)^{1/2})] + bI$, where z_+ and z_- are the cation and anion charges, here equal to $+1$ and -1, respectively, $\gamma_{\pm}$ is the average activity coefficient of the ions ($\gamma_{\pm} = (\gamma_+\gamma_-)^{1/2}$), A and B are constant parameters that depend on the dielectric constant of the solvent and on temperature, a is the effective radius of the hydrated ion, and I the ionic strength of the solution. This equation, which usually holds up to at least 1 M salt solutions, was proposed by Robinson and Stokes 50 years ago.[9]

We will here consider an illustrative theoretical and experimental model system. The system comprises an equilibrium finite volume self-assembled two-phase system of a phospholipid in salt water.

* To whom correspondence should be addressed. E-mail: tavares@eq.ufrj.br.
[†] Linköping University.
[‡] University of Regensburg.
[§] Universita di Cagliari-CSGI Cittadella Monserrato.
[⊥] Programa de Engenharia Química, COPPE, Universidade Federal do Rio de Janeiro.
[#] Escola de Química, Universidade Federal do Rio de Janeiro.
[¶] University of Florence.
[▽] Australian National University Canberra.

10.1021/jp809051j CCC: $40.75
Published on Web 05/14/2009

Aqueous dispersions of dioctanoyl-phosphatidylcholine (diC_8PC) phase separate upon cooling. The upper coexistence curve is obtained by recording the cloud point temperature as a function of the lipid mole fraction. The maximum corresponds to the critical upper consolute temperature T_c and to the critical lipid mole fraction x_c. Upon phase separation, two phases coexist; the upper phase consists of a diluted micellar solution of the lipid, while the bottom phase is highly viscous (it looks like a gel) and contains very large entangled wormlike aggregates.[10] The addition of different single sodium salts results in a consistent shift of the coexistence curve and in a variation of its skewness. These changes follow the Hofmeister series and are particularly relevant in the presence of soft, highly polarizable species, such as I^- and SCN^- (monovalent anions with large size).[8] The concentrations of the anions in the two coexisting phases have been measured through ion chromatography and show that Br^- and NO_3^- accumulate in the lipid-rich bottom phase, resulting in an asymmetric partition between the two coexisting phases, while F^- ions distributes almost evenly.

In the present contribution, we will show that it is the anions with higher polarizability that accumulate to a much higher degree in the dense phase than anions with lower polarizability. That is, the previously neglected nonelectrostatic ion binding to micelle surfaces in the two-phase system provides a reasonable mechanism for the observed asymmetric ion partitioning.

The specific ion partitioning that occurs with red cells parallels this situation; a concentrated phase with hemoglobin of high surface area and available for specific ion adsorption is separated from a finite volume of overall physiological saline.

We can then speculate that our model results provide some hint into additional equilibrium contributors to "ion pumps". The source of this specific ion binding lies at least partly in the ion-specific nonelectrostatic (NES) forces and short-range hydration forces missing from classical theories of electrolytes.[5−12]

We will show theoretically how different anions accumulate in a specific way in a finite reservoir colloidal solution. Each colloidal particle binds a defined number of anions, which can be calculated using a modified Poisson−Boltzmann theory. The two phases have finite volumes, that is, there is no infinite reservoir as in classical theory. To do so, we maintain ion balance in the system, keeping the number of ions constant during the calculation. The total anion concentration in the dense phase is equal to the number of ions bound to each colloidal particle multiplied by the concentration of colloidal particles plus the background salt concentration. More polarizable anions give rise to higher anion concentrations in the dense phase. We then relate these results to the experimental results[8] that coexisting phases have different anion concentrations at the same overall salt concentration.

2. Theory Section

We consider a model system with a finite number (N_{cell}) of neutral (i.e., uncharged) colloidal particles (micelles) in a dense phase. These are treated as independent spherical particles each surrounded by an ion cloud. We use a cell model to study this system (see Figure 1). The ion concentration at the boundary between two cells is taken to be equal to the bulk concentrations in the two phases. This is so there is no Donnan potential set up between the two phases when the colloidal particles, which are the only species that cannot move freely between the two phases, are uncharged. Each cell is analyzed using a modified Poisson−Boltzmann theory in spherical coordinates

$$\frac{\varepsilon_w \varepsilon_0}{r^2}\frac{d}{dr}\left(r^2\frac{d\varphi}{dr}\right) = -e[c_+(r) - c_-(r)] \quad (1)$$

with the ion concentrations given by

$$c_\pm(r) = c_{0,\pm}\exp[-(\pm e\varphi + U_\pm(r))/(kT)] \quad (2)$$

Here, φ is the self-consistent electrostatic potential; $c_{0,\pm}$ are the bulk ion concentrations, and $U_\pm$ are the nonelectrostatic interaction potentials experienced by the ions when they are close to a colloidal particle. The boundary conditions follow from global charge neutrality along with the condition of no charge at the cell boundary. The electric field at the charge neutral colloidal particle surface is therefore 0. The NES potential corresponds to the van der Waals dispersion interaction obtained from Lifshitz theory.[11,12] In spherical coordinates, the expression used to calculate $U_\pm(r)$ is[5c]

$$U_\pm(r) = -\frac{B_\pm}{(r - r_p)^3\left[1 + \frac{(r - r_p)^3}{2r_p^3}\right]} \quad \text{for} \quad r > r_{ion} + r_p \quad (3)$$

where r_p is the colloidal particle (micelle) radius, r_{ion} is the ion radius, and $B_\pm$ is the dispersion interaction coefficient obtained from Lifshitz theory. The specified number of ions $N_{i,0}$ in the system is kept constant during the calculation. This condition is satisfied by means of the following ion balance

$$N_{i,0} = c_{i,0}\left[\left(V_t - N_{cell}\frac{4}{3}\pi\cdot R_{cell}^3\right) + 4\pi\cdot N_{cell}\int_{r_p}^{R_{cell}}\exp\left(\frac{-\varphi e z_i - U_i}{kT}\right)r^2 dr\right] \quad (4)$$

Here, $V_t = V_1 + V_2$ is the total volume of the system, N_{cell} is the number of micelles in phase 2, r_p is the radius of the micelle (colloidal particle), and $R_{cell} = D_{cell}/2$ is the radius of the cell in the model. The first term on the right-hand side corresponds to the ions far from the micelles, where the NES interactions do not have any influence (outside of the double layer). The integral in the second term stands for the ions near the micelles. Near a micelle, due to NES interactions, there is a higher concentration of ions than that in the micelle free phase; therefore, this excess of ions is subtracted from the bulk. The bulk concentra-

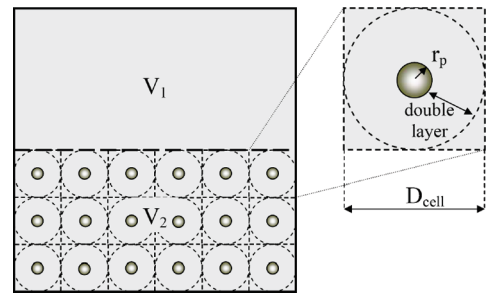

Figure 1. Micelle model: phase 1 (micelle free phase) contains an electrolyte solution, and phase 2 contains micelles immersed in the same electrolyte solution. The total number of ions in the system is kept fixed.

TABLE 1: Dispersion Interaction Coefficients $B_{\pm}$ (10^{-50} J m^3) Used in Figure 3

model	Na^+	Cl^-	Br^-	I^-
FWT et al. water; colloid and α[11]	−0.454	−3.576	−4.438	−5.712
FWT et al. colloid and water;[11] ab initio α[13]	−0.4971	−7.022	−7.8389	−12.278
FWT et al. colloid;[11] PW water;[14] ab initio α[13]	−0.4482	−6.859	−7.6271	−12.052
FWT et al. colloid;[11] Nir water;[15] ab initio α[13]	−0.5744	−7.765	−8.71	−13.433

tion $c_{i,0}$ is determined by solving the differential algebraic system formed by eqs 1−4 iteratively.

In this approach, we consider that the colloidal particle concentration is sufficiently low that the mean separation between two colloidal nanoparticles (micelles) is much larger than the Debye length.

We consider different approaches in the calculation of ion polarizabilities and dispersion interaction coefficients $B_{\pm}$. Ion polarizabilities as a function of imaginary frequency have been calculated by ab initio quantum chemistry.[13] Previous studies[11] used a single-mode model of the polarizability with the characteristic frequency estimated from the ionization potential of the ion. Instead, the ab initio polarizabilities in principle contain all contributing modes. Dispersion coefficients were calculated at $T = 25$ °C by summing over temperature-dependent imaginary frequencies $\omega_n = 2k\pi Tn/\hbar$,

$$B_{\pm} = \frac{-kT}{4}\sum_{n=0}(2-\delta_{0,n})\frac{\alpha_{\pm}(i\omega_n)\,[\varepsilon_c(i\omega_n)-\varepsilon_w(i\omega_n)]}{\varepsilon_w(i\omega_n)\,[\varepsilon_c(i\omega_n)+\varepsilon_w(i\omega_n)]} \quad (5)$$

where $\varepsilon_w(i\omega)$ and $\varepsilon_c(i\omega)$ are the dielectric permittivity spectra for water and colloid, respectively. A single-mode model for the dielectric function of the colloid was employed[11]

$$\varepsilon_c(i\omega) = 1 + \frac{n^2-1}{1+(\omega/\omega_I)^2} \quad (6)$$

with $n = 1.6$ and frequency ω_I taken from an estimate of the ionization energy,[11] 3×10^{15} Hz. Refractive index n and frequency ω_I were chosen in order to provide consistency with previous studies of biological colloids.[11] A number of models for the description of the dielectric spectrum of water were compared, including a single-mode model (eq 6) with the characteristic frequency derived from the ionization energy of water ($n = 1.333$, $\omega_I = 3 \times 10^{15}$Hz, and taking $\varepsilon_w(i\omega) = 78.5$ when $\omega = 0$).[11] The other models for the dielectric spectrum of water due to Parsegian and Weiss (PW)[14] and due to Nir[15] were experimentally derived with multiple modes and are therefore expected to be more reliable than the single-mode ionization potential model. The calculated $B_{\pm}$ dispersion coefficients are given in Table 1. Ab initio polarizabilities provide a large correction to the B values of the anions compared with those calculated using the single-mode ionization potential (IP) model of polarizability, the ab initio estimates being more than twice as large as the IP estimates. The reason for the increased B values is illustrated by the dynamic polarizabilities for Br^-, shown in Figure 2. Although the ab initio static polarizability of Br^- at 0 frequency is lower than the value used in the single-mode IP model, the single-mode model drops to 0 at much lower frequencies than the ab initio model. That is, ab initio polarizabilities provide a much larger high-frequency tail than the single-mode model, resulting in the increase in B values. The larger ab initio high-frequency tail is seen in all ions, including metal cations. The effects of nonelectrostatic interactions will therefore be much greater than those seen in previous studies. Further, we note that the description of the dielectric properties of water also makes a difference, albeit relatively small, with Nir's model, giving slightly larger B values than the Parsegian−Weiss model. Because of the abundance of water in biological systems, the right characterization of its dielectric properties may well be critical.

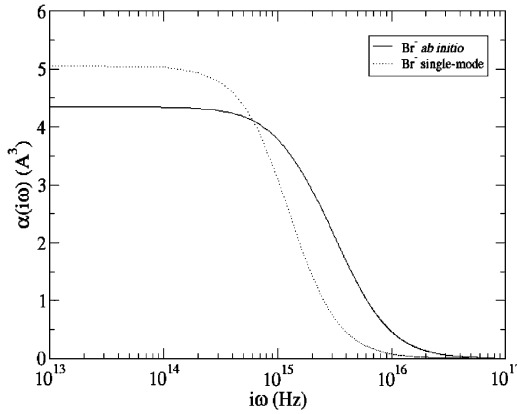

Figure 2. The dynamic polarizability $\alpha(i\omega)$ for Br^-. Two models are compared, the ab initio calculation (solid line) and the single-mode model with the characteristic frequency given by the ionization potential of the ion (dotted line).

Nir's model employs four terms in the IR region and one in the UV, whereas the Parsegian−Weiss model employs five and six, respectively, plus one in the microwave region corresponding to the dielectric constant. However, even for the same set of experimental data, the procedure used to fit the dielectric function can yield significantly different results, as discussed by Dagastine et al.[16]

3. Results

Figure 3 shows the variation of the concentration ratio between the upper (1) and lower (2) phases for the investigated anions as a function of the ion polarizability in solution. In our model, we have considered $V_1 = V_2 = 0.5$ cm^3, $r_p = 3$ nm, and a concentration of cells of 2 mM in the dense phase ($N_{cell} = 6 \times 10^{17}$; $D_{cell} = 9.4$ nm).

In Figure 3a, we compare the experimental results reported in ref 8 with the micelle model presented here using ab initio polarizabilities together with Nir's model for the dielectric spectrum of water and Tavares's model for colloidal particles (correspondent parameters are presented in the last line of Table 1). We see that with this simple model, we can get the right trends. The more polarizable the ion, the more it tends to accumulate in the dense phase, adsorbing to the micelle surfaces. This is in agreement with experiment.[8] In Figure 3b, we compare different models (parameters are presented in Table 1). The difference in the quantitative results is partly due to the difficulty in determining the ion polarizabilities and the dielectric functions for this system. These parameters are necessary to calculate the ion dispersion interaction coefficients. We emphasize that there is no adjustable parameter in our model.

The model calculations are, strictly speaking, made for micelles and are therefore indicative only of the real experimental system of Lagi et al.[8] However, this system provides a useful model for entangled worms as they possess a high surface area for specific ion adsorption.The same ideas could be applied

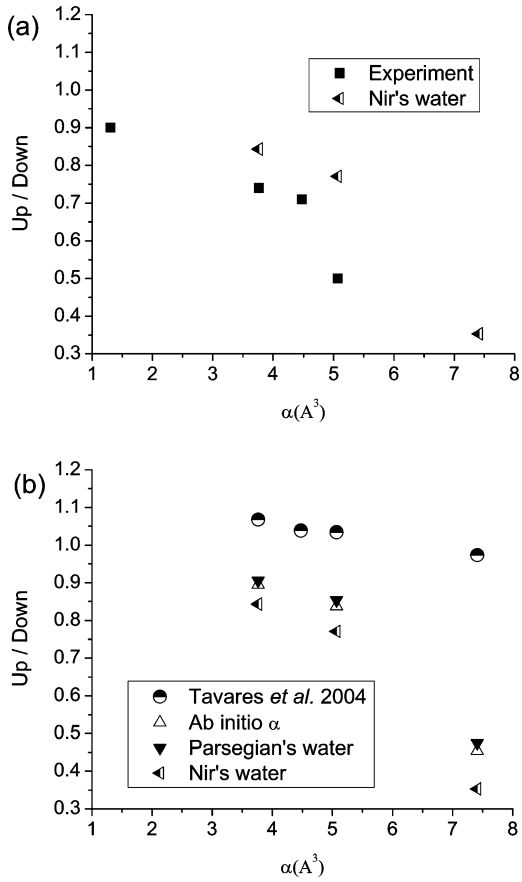

Figure 3. The variation of the concentration ratio between the upper and lower phase for the investigated anions as a function of the ion polarizability in solution. (a) Comparison between experimental results taken from Lagi et al.[8] and the model considering Nir's water with ab initio polarizabilities. (b) Comparison between different models (theoretical dispersion interaction coefficients are given in Table 1).

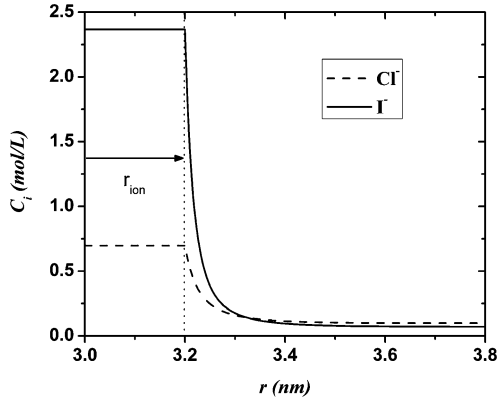

Figure 4. Anion profiles near a micelle in the system shown in Figure 1, with an electrolyte solution containing NaCl and NaI in the same quantity. The plateau between 3 and 3.2 nm corresponds to the ion radius, and 3 nm is the micelle radius.

for other systems with high surface area. The spherical model mimics, for example, the biological system of hemoglobin in a red cell.

In Figure 4, we show the ion profiles for a system containing a mixed electrolyte containing NaCl and NaI with the same number of chloride and iodide ions, using the model of Tavares et al.[11] for the dielectric function of colloidal particles but with new ab initio polarizabilities. We can see clearly that the iodide ions accumulate in a higher concentration near the micelle interface. There is adsorption due to NES interaction similar to that described by Lima et al.[17] This excess of ions near the micelles gives rise to a considerable difference between the mole ratios of different ions. The more polarizable the ion, the more it tends to accumulate in the dense phase, adsorbing to the micelle surfaces. This is in agreement with experiment.[8]

The ion balance results in a bulk concentration of chloride greater than that for iodide because a higher number of iodide ions adsorb to the micelle interface, migrating from the bulk.

4. Conclusion

The anion-specific partitioning observed with an equilibrium two-phase system of phospholipids cannot be explained by a classical electrostatic theory. It is explainable when dispersion forces acting on ions are taken into account. The same mechanism must operate in any system of lipids, proteins or polymers, compartmentalized by a membrane or segregated by equilibrium phase separation. With charged macroions like hemoglobin, the mechanism will lead additionally to a potential across the membrane or interface. How much this mechanism contributes to active ion pumps remains to be explored. We are working on a new model for a two-phase system with a membrane, based on the model presented in this manuscript. In the new model, additional equations arise from the chemical potential equilibrium in the system, and the Donnan potential follows naturally. This will enable us in the near future to investigate how much the effect studied here contributes to ion partitioning in red blood cells.

Acknowledgment. We thank the Swedish Research Council and Swedish Royal Academy of Science, the German Arbeitsgemeinschaft industrieller Forschungvereinigungen Otto von Guericke e.V. (AiF), and FAPERJ, CAPES, and CNPq (the last three Brazilian Agencies) for financial support and the Australian Research Council's *Discovery Projects* funding scheme.

References and Notes

(1) (a) Zhang, Y.; Cremer, P. S. *Curr. Opin. Colloid Interface Sci.* **2006**, *10*, 658. (b) Ninham, B. W.; Yaminsky, V. *Langmuir* **1997**, *13*, 2097.
(2) Freedman, J. C. In *Cell Physiology Sourcebook*, 2 ed.; Sperelakis, N., Ed.; Academic Press: San Diego, CA, 1998.
(3) Skou, J. C. *Biochim. Biophys. Acta* **1957**, *23*, 394.
(4) Edelmann, L. *Cell. Mol. Biol.* **2005**, *51*, 725.
(5) (a) Ninham, B. W.; Boström, M. *Cell. Mol. Biol.* **2005**, *51*, 803. (b) Boström, M.; Williams, D. R. M.; Ninham, B. W. *Phys. Rev. Lett.* **2001**, *87*, 168103. (c) Boström, M.; Williams, D. R. M.; Ninham, B. W. *Langmuir* **2002**, *18*, 6010.
(6) Lo Nostro, P.; Ninham, B. W.; Lo Nostro, A.; Pesavento, G.; Fratoni, L.; Baglioni, P. *Phys. Biol* **2005**, *2*, 1.
(7) Petrache, H. I.; Kimchi, I.; Harries, D.; Parsegian, V. A. *J. Am. Chem. Soc.* **2007**, *12*, 11546.
(8) Lagi, M.; Lo Nostro, P.; Fratini, E.; Ninham, B. W.; Baglioni, P. *J. Phys. Chem. B* **2007**, *111*, 589.
(9) Robinson, R. A.; Stokes, R. H. *Electrolyte Solutions*; 2nd ed.; Butterworths Scientific Publications: London 1959; p, 231.
(10) Lo Nostro, P.; Murgia, S.; Lagi, M.; Fratini, E.; Karlsson, G.; Almgren, M.; Monduzzi, M.; Ninham, B. W.; Baglioni, P. *J. Phys. Chem. B* **2008**, *112*, 12625.
(11) Tavares, F. W.; Bratko, D.; Blanch, H.; Prausnitz, J. M. *J. Phys. Chem. B* **2004**, *108*, 9228.
(12) Boström, M.; Deniz, V.; Franks, G. V.; Ninham, B. W. *Adv. Colloid Interface Sci.* **2006**, *123*−*126*, 5.
(13) (a) Adamovic, I.; Gordon, M. *Mol. Phys.* **2005**, *103*, 379387. (b) More recent work will come from Parsons, D. F.; Ninham, B. W. **2008**.
(14) Parsegian, V. A.; Weiss, G. H. *J. Colloid Interface Sci.* **1981**, *81*, 285.
(15) Nir, S. *Prog. Surf. Sci.* **1976**, *8*, 1.
(16) Dagastine, R. R.; Prieve, D. C.; White, L. R. *J. Colloid Interface Sci.* **2000**, *231*, 351.
(17) Lima, E. R. A.; Boström, M.; Horinek, D.; Biscaia, E. C., Jr.; Kunz, W.; Tavares, F. W. *Langmuir* **2008**, *24*, 3944.

JP809051J